

Probing Axions via Light Circular Polarization and Event Horizon Telescope

Fazlollah Hajkarim

University of Oklahoma

PASCOS Conference, Irvine, June 28, 2023

Based on S. Shakeri, F. H., [arXiv:2209.13572](https://arxiv.org/abs/2209.13572) , JCAP 04 (2023) 017

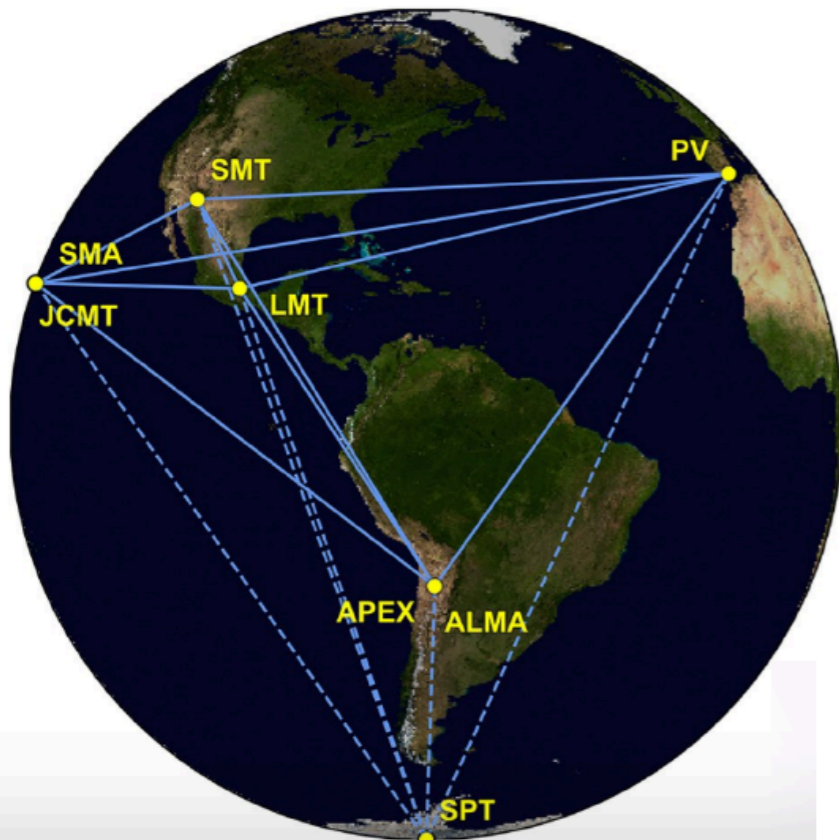
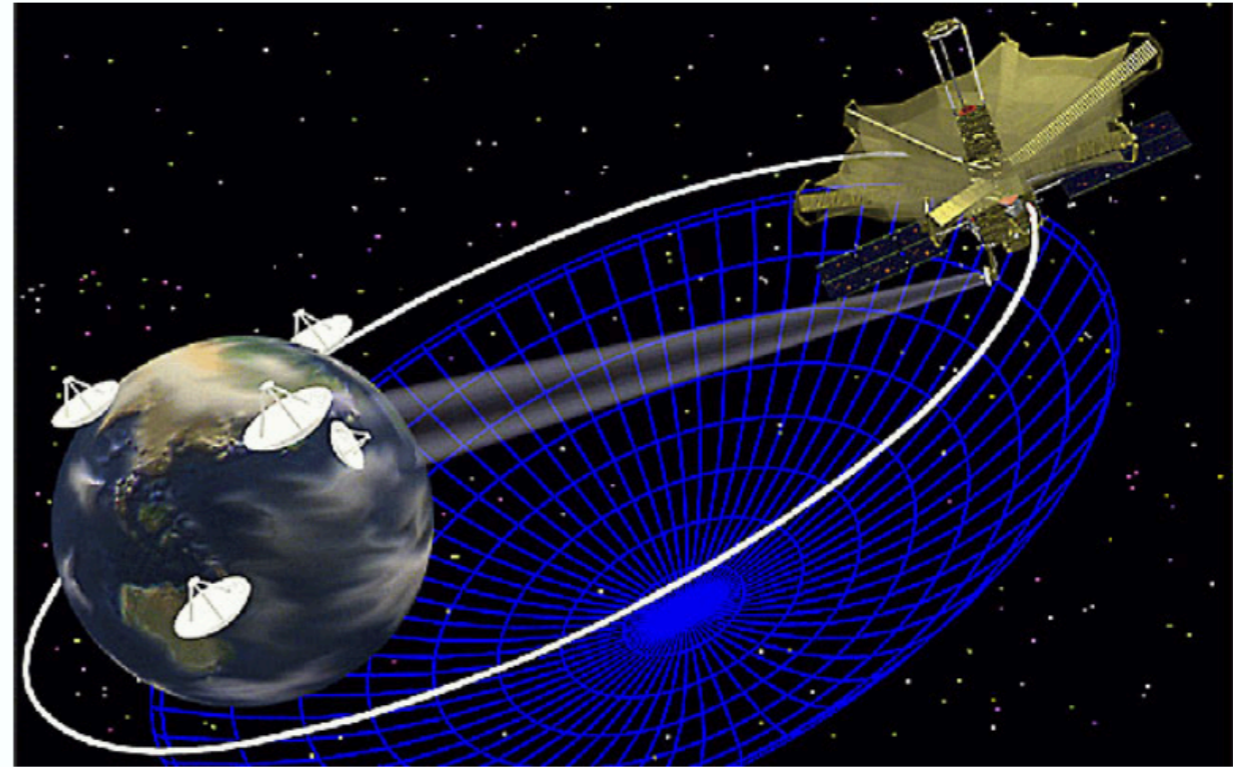
Overview

- Vacuum solutions of General Relativity results in the presence of Black Holes. BH properties depend on the boundary conditions for the GR solutions.
- Kerr BH predicted in 1963 describes massive spinning objects as one of the realistic solutions of GR
- The observation of a BH at galactic centre by Event Horizon Telescope (EHT) was one of the confirmation of GR beyond the solar system and a confirming evidence for the presence of BH especially supermassive BH (SMBH) at the centre of galaxies
- Also, observation of gravitational wave from binary BH mergers by LIGO was another triumph of GR at the galactic/cosmological scale
- These new experiments can also indirectly constrain/observe the physics beyond the standard model
- Axion (like particles) as a BSM physics candidate (for dark matter) due to the interaction with photons or indirect impact on massive objects can be probed with EHT or GW experiments

We studied the impact of axion on light polarization around a SMBH!

Event Horizon Telescope

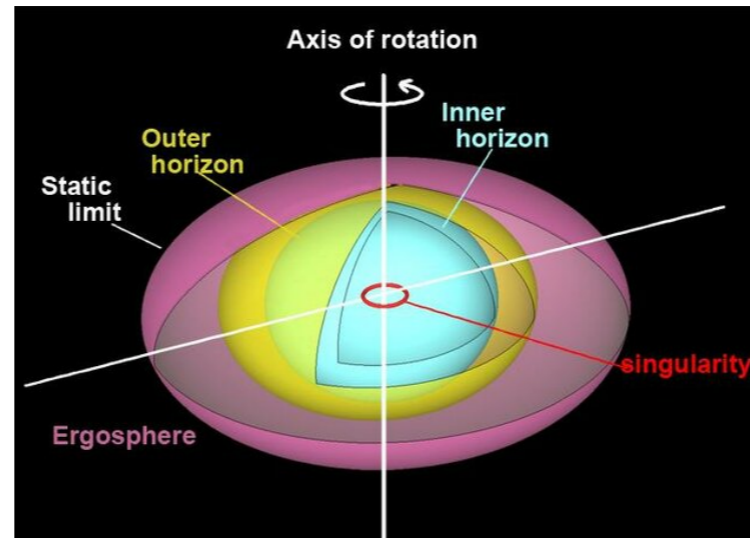
The Detection Method of EHT: behaves like virtual Earth-sized telescope using very long baseline interferometry



At frequencies of about 230 GHz (wavelength of 1.3 mm), Earth-size baselines can resolve an apple on the Moon.

Kerr Geometry

In reality black holes are spinning objects. They can be well described by Kerr metric.



<https://www.geraintflewlewis.com/post/black-holes-and-the-mystery-of-the-ergosphere>

$$ds^2 = - \left(1 - \frac{2M_{BH}r}{\Sigma} \right) dt^2 - \frac{4aM_{BH}r \sin^2 \theta}{\Sigma} dt d\phi + \frac{\Sigma}{\Delta} dr^2 + \Sigma d\theta^2 + \left(r^2 + a^2 + \frac{2a^2 M_{BH} r \sin^2 \theta}{\Sigma} \right) \sin^2 \theta d\phi^2$$

$$\Sigma = r^2 + a^2 \cos^2 \theta \quad \Delta = (r - r_+)(r - r_-) \quad r_{\pm} = M_{BH} \pm \sqrt{M_{BH}^2 - a^2}$$

$a = J/M$ is the angular momentum per unit mass of the black hole.

Superradiance

Superradiance conditions are discovered under which waves incident on a rotating black hole can extract energy and angular momentum from the black hole, leading to amplification and scattering of the waves - [Zeldovich, Press, Teukolsky \(1970s\)](#).

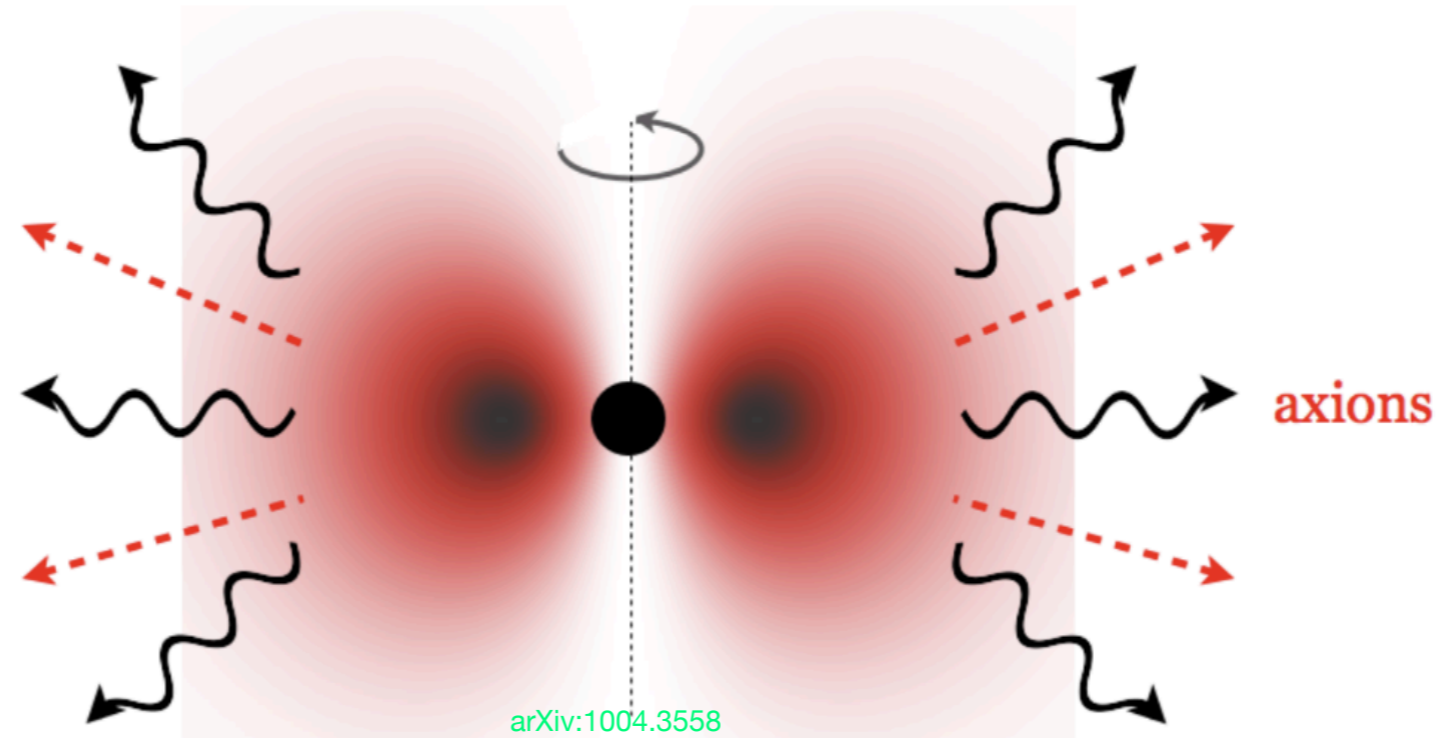
This occurs when the energy and angular momentum of the incident particles satisfy certain conditions. Axions as dark matter candidates can interact with black holes. Axions can be produced in the intense environment of a black hole's accretion disk and affect its properties. They can also interact with electromagnetic fields, leading to the conversion of photons into axions and vice versa.

The condition for superradiance around a rotating black hole is: $\omega < m\Omega$

- ω : The frequency of the incident wave or particle.
- m : An integer representing the azimuthal mode number.
- Ω : The angular velocity of the rotating black hole.

The condition $\omega < m\Omega$ states that the frequency of the incident wave or particle must be lower than the product of the azimuthal mode number and the angular velocity of the black hole. This condition ensures that the energy and angular momentum of the wave can be extracted by the black hole, leading to superradiant amplification.

Axion Density Around a SMBH



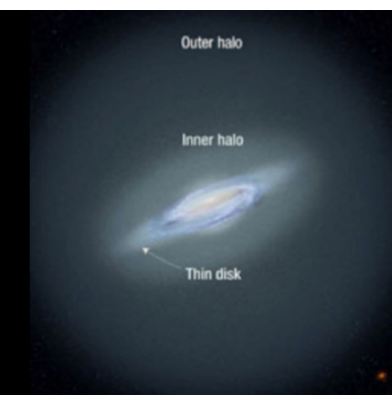
$$\rho_a|_{\max} = \frac{1}{2}m_a^2 a^2|_{\max} = \frac{1}{2}m_a^2 f_a^2 \approx 3.83 \times 10^{11} \left(\frac{m_a}{10^{-20}\text{eV}} \right)^2 \left(\frac{f_a}{10^{16}\text{GeV}} \right)^2 \left[\frac{\text{GeV}}{\text{cm}^3} \right]$$

★ The superradiant instability depends on the dimensionless product of the BH mass and axion mass as

$$M_{\text{BH}} m_a = 4.65 \times 10^{-1} \left(\frac{M_{\text{BH}}}{6.2 \times 10^9 M_{\odot}} \right) \left(\frac{m_a}{10^{-20} \text{eV}} \right)$$

Dark Matter Local Density in Halo:

$$\rho_{\text{DM}} \sim 0.4 \frac{\text{GeV}}{\text{cm}^3}$$



[arXiv:2209.13572](https://arxiv.org/abs/2209.13572)

Light Polarization

Linear Polarization:

- Intrinsic to the emission process: the synchrotron emission, Bremsstrahlung, curvature radiation, etc.
- Due to the propagation effect: the Compton scattering, plasma effect, etc.

But usual scattering process (like Compton scattering)
can not produce circular polarization!

Circular Polarization:

- Parity violating interactions
- Intrinsic asymmetric distribution of left- and right-handed components in target beams
- The presence of an anisotropic background in the medium

Axion-Photon Interaction is Parity Violating!

Light Polarization

Stokes parameters: I (the total intensity), Q and U (linear polarization), and V (the circular polarization):

$$I = \rho_{11} + \rho_{22} \equiv \langle \dot{A}_x^2 \rangle + \langle \dot{A}_y^2 \rangle, \quad Q = \rho_{11} - \rho_{22} \equiv \langle \dot{A}_x^2 \rangle - \langle \dot{A}_y^2 \rangle, \quad U = \rho_{12} + \rho_{21} \equiv \langle 2\dot{A}_x\dot{A}_y \cos(\phi_x - \phi_y) \rangle, \quad V = i(\rho_{12} - \rho_{21}), \equiv \langle 2\dot{A}_x\dot{A}_y \sin(\phi_x - \phi_y) \rangle$$

$$\rho = \frac{1}{2} \begin{pmatrix} I + Q & U - iV \\ U + iV & I - Q \end{pmatrix}$$

$$\hat{\mathcal{D}}_{ij}(\mathbf{k}) = \hat{a}_i^\dagger(\mathbf{k})\hat{a}_j(\mathbf{k})$$

$$(2\pi)^3 2k^0 \delta^{(3)}(0) \frac{d}{dt} \rho_{ij}(\mathbf{k}) = i \langle [\hat{\mathcal{H}}_{int}(t), \hat{\mathcal{D}}_{ij}(\mathbf{k})] \rangle - \frac{1}{2} \int_{-\infty}^{+\infty} dt \left\langle \left[\hat{\mathcal{H}}_{int}(t), [\hat{\mathcal{H}}_{int}(0), \hat{\mathcal{D}}_{ij}(\mathbf{k})] \right] \right\rangle$$

$$A_\mu(x) \equiv A_\mu^+(x) + A_\mu^-(x) = \int \frac{d^3\mathbf{k}}{(2\pi)^3 2\omega_\gamma} \left[\hat{\mathbf{a}}_i(\mathbf{k}) \epsilon_{i\mu}(\mathbf{k}) e^{-ik \cdot x} + \hat{\mathbf{a}}_i^\dagger(\mathbf{k}) \epsilon_{i\mu}^*(\mathbf{k}) e^{ik \cdot x} \right]$$

Coherently Oscillating Axion Field

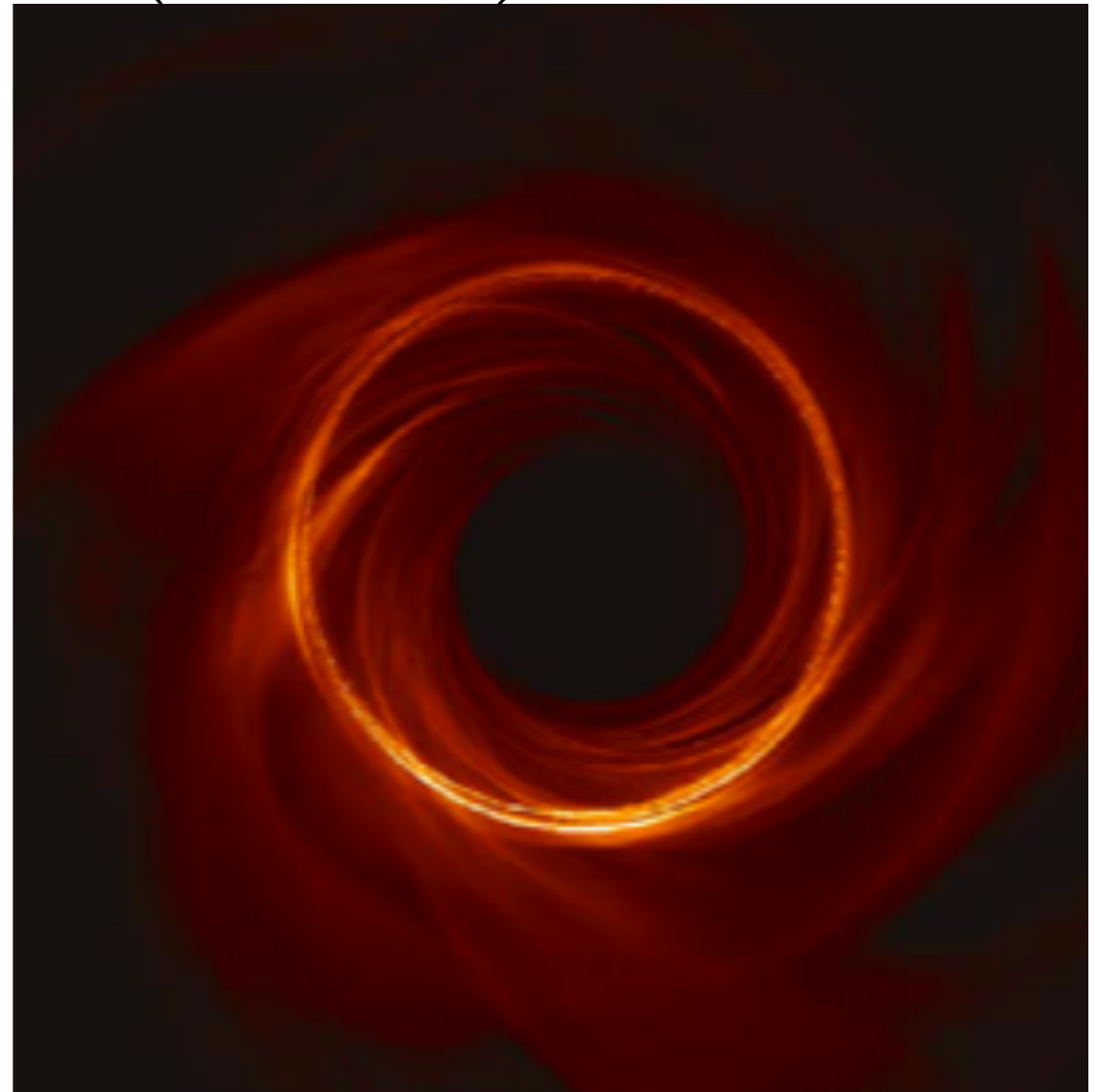
$$\mathcal{L} = -\frac{1}{4}F_{\mu\nu}F^{\mu\nu} + \frac{1}{2}\left(\partial_{\mu}a\partial^{\mu}a - m_a^2a^2\right) + \frac{1}{4}g_{a\gamma}aF_{\mu\nu}\tilde{F}^{\mu\nu}$$

$$g_{a\gamma} \equiv \frac{c_{a\gamma}}{2\pi f_a} \quad c_{a\gamma} \equiv \alpha_{\text{em}} \left(\frac{E}{N} - 1.92 \right)$$

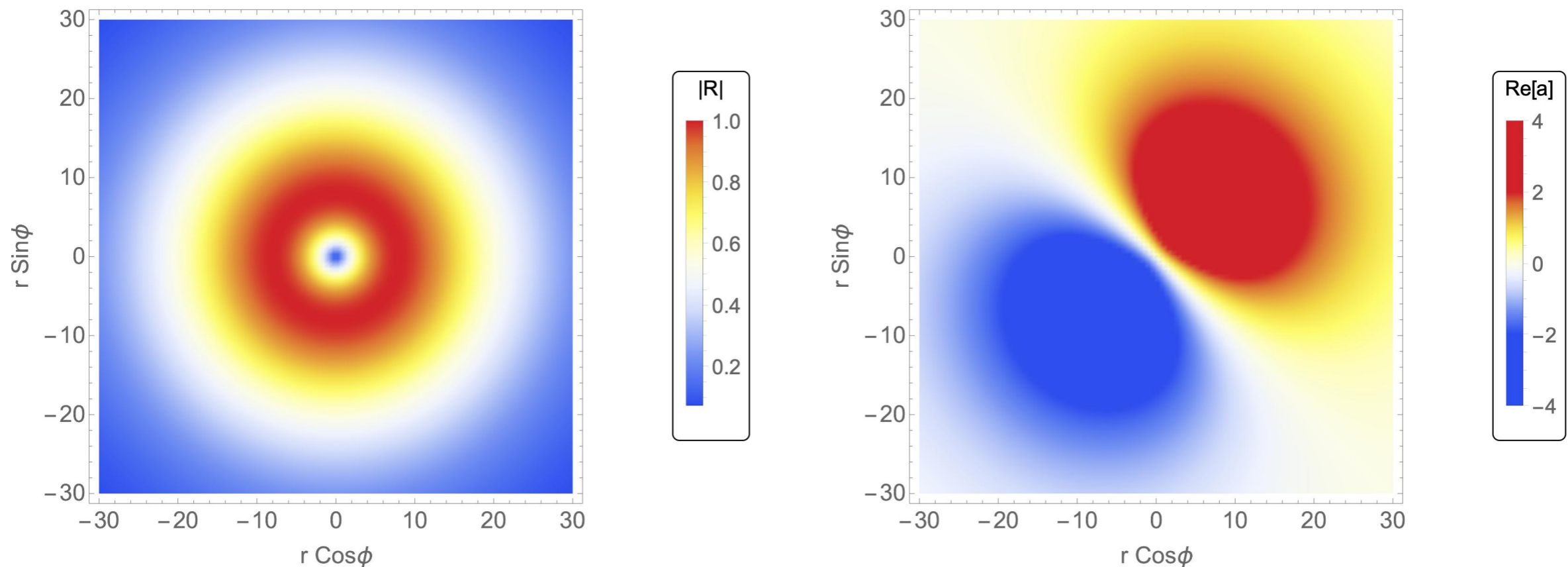
$$a(\vec{r}, t) \equiv \Re e \left(a_0(r) e^{i(\mathbf{p}\cdot\mathbf{r} - \omega t)} \right) \equiv a_0(r) \cos [m_a t + \delta(r)]$$

$$T \simeq \frac{2\pi}{m_a} \simeq 4.2 \times 10^{-9} \left(\frac{10^{-6} \text{eV}}{m_a} \right) s$$

$$r_g \equiv GM_{BH} = 2.97 \times 10^{-4} \text{pc} \left(\frac{M_{BH}}{6.2 \times 10^9 M_{\odot}} \right)$$



Axion Field Around the Black Hole



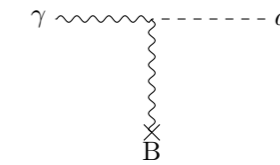
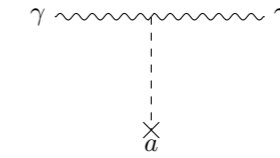
Axion field around the black hole is shown. The left and right panels are for the radial part of axion field $|R|$ (scaled to its maximum) and its real part $\text{Re}[a]$ scaled to its numerical factor at $\theta = \pi/2$ from following equations with $l = 1$, respectively. The radial distance has been scaled to $r_{cloud} \sim 8$ which means that $M_{BH}m_a^2 = 0.25$.

$$\square a = m_a^2 a \rightarrow a(t, r, \theta, \phi) = e^{im\phi} S_{lm}(\theta) e^{-i\omega t} R_{nl}(r) \rightarrow R_{nl}(r) = A_{nl} g(\tilde{r}), \quad g(\tilde{r}) = \tilde{r}^l e^{-\tilde{r}/2} L_n^{2l+1}(\tilde{r}), \quad \tilde{r} = \frac{2rM_{BH}m_a^2}{l+n+1}$$

$$a(t, r, \theta, \phi) = \sqrt{\frac{3M_S}{4\pi \times 24M_{BH}}} (M_{BH}m_a^2)^2 g(\tilde{r})^{n=0, l=1} \cos(\phi - \omega_R t) \sin \theta$$

Polarisation Angle of Linearly Polarized Emission

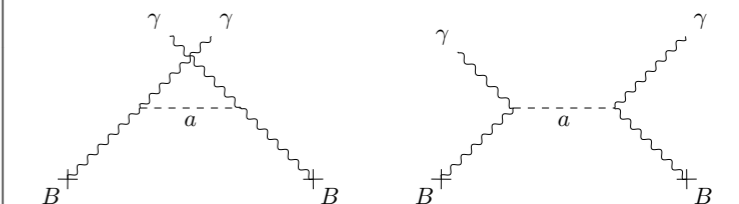
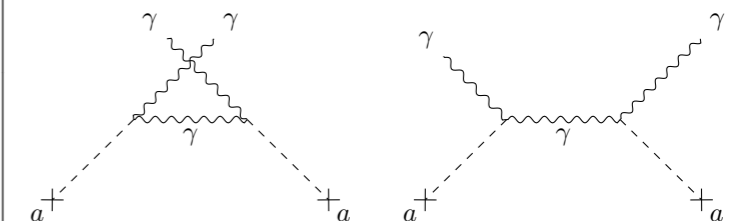
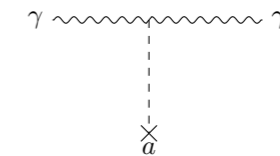
Polarization Angle $\Delta\psi$ of Linearly Polarized Emission	
Physical Process	The Axion Polarization Angle
Propagation of Photons in an Axion Background	$\Delta\psi = g_{a\gamma}\Delta a(\vec{r}, t)$
Axion-photon Conversion in a Magnetic Field	$\Delta\psi = \frac{1}{4}P_{\gamma\rightarrow a}\sin 2\alpha$



[arXiv:2209.13572](https://arxiv.org/abs/2209.13572)

Sources of Circular Polarization

Sources of Circular Polarization	
Physical Process	Form of the Axion Polarization Term
Axion Induced Propagation Effect	$\Pi_V = \frac{2\pi g_{a\gamma}\dot{a}}{\omega_\gamma} + \mathcal{O}(g_{a\gamma}^2)$
Scattering of Photon from Axion	$\Pi_V = 8g_{a\gamma}^2 a_0^2 \frac{\omega_\gamma}{m_a^2 - 4\omega_\gamma^2} (\mathbf{p}_x^2 + \mathbf{p}_y^2) r$
Photon Scattering from a Magnetic Field	$\Pi_V = \frac{\omega_\gamma g_{a\gamma}^2}{m_a^2} (B_x^2 + B_y^2) r$



Contribution of Different Axion Channels to Light Polarization around SMBH

The polarization angle can be defined in terms of Stokes parameters as

$$\psi = \frac{1}{2} \arctan \frac{U}{Q}$$

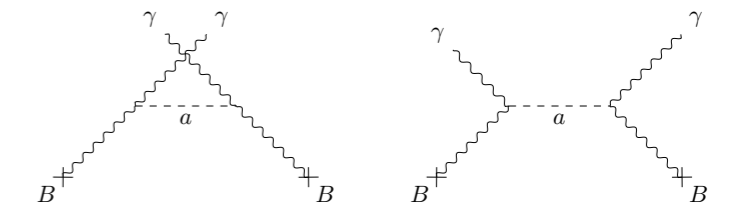
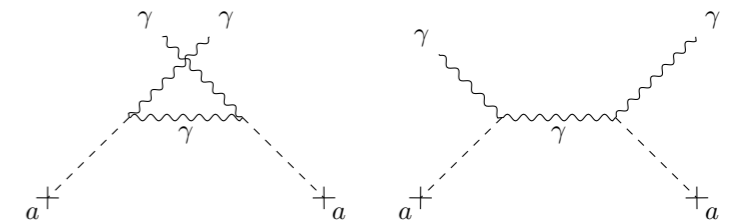
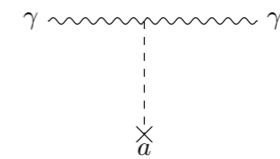
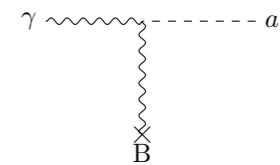
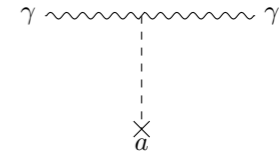
$$\Delta\psi|_{\max} \approx -8.20 \times 10^{-3} c_{a\gamma} \cos(\phi - m_a t) \sin \theta$$

$$\Delta\psi|_{\max} \approx 7.28 \times 10^{-5} \cdot \left(g_{a\gamma} / 10^{-12} \text{GeV}^{-1} \right)^2 \rightarrow f_a = 10^{15} \text{GeV} \rightarrow \Delta\psi|_{\max} \approx 1.16 \times 10^{-8} c_{a\gamma}^2 \text{ }^\circ$$

$$\Pi_V = \frac{2\pi g_{a\gamma} \dot{a}}{\omega_\gamma} = 5.41 \times 10^{-19} c_{a\gamma} \left(\frac{m_a}{10^{-20} \text{eV}} \right) \left(\frac{230 \text{GHz}}{\nu_\gamma} \right) \sin(\phi - m_a t) \sin \theta$$

$$\Pi_V \equiv \frac{|V|}{I} = |\sin(\Omega t)| \approx |\Omega| t = 4.94 \times 10^{-25} c_{a\gamma}^2 \left(\frac{r}{r_g} \right)$$

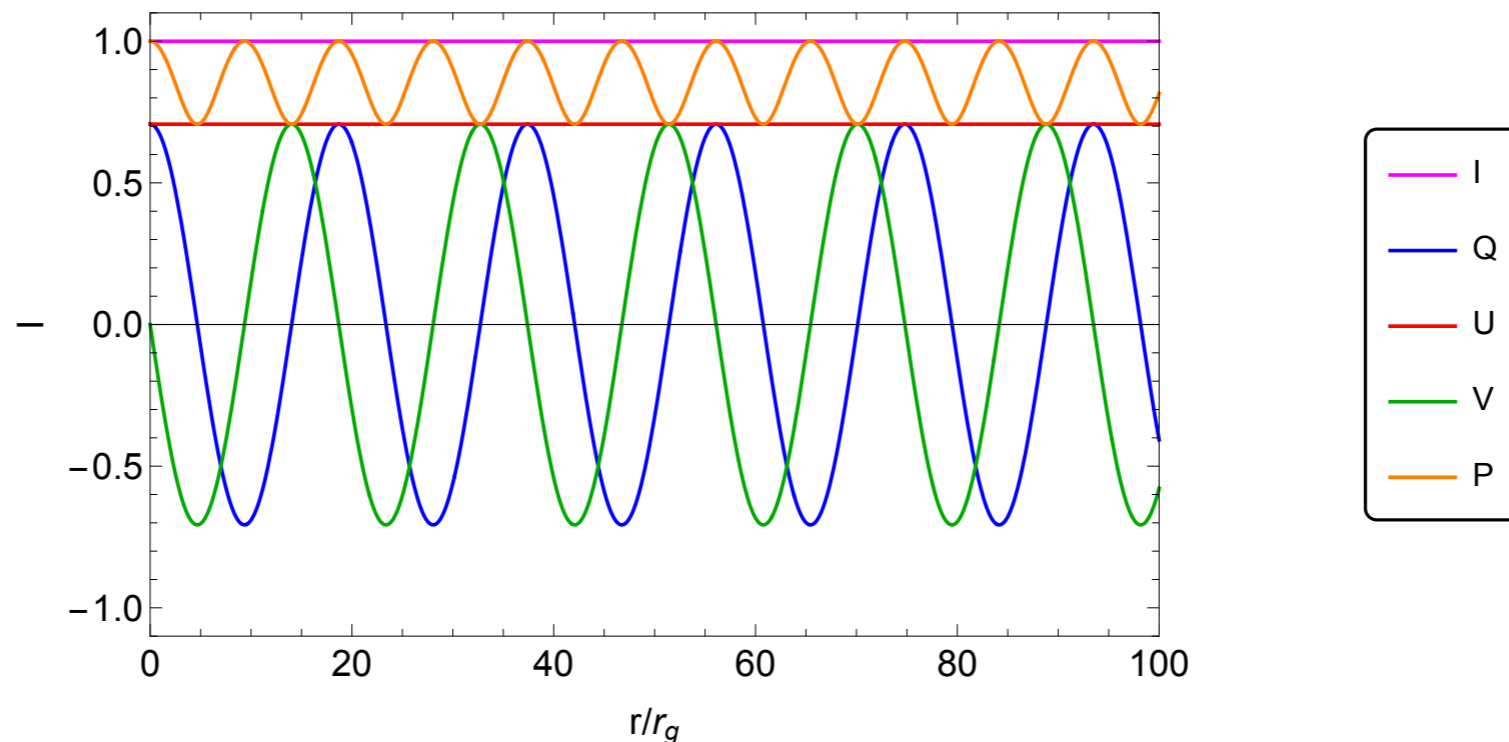
$$\star \Pi_V \equiv \frac{|V|}{I} = |\sin(\Omega t)| \approx |\Omega| t = 0.85 \left(\frac{c_{a\gamma}}{0.1} \right)^2 \left(\frac{\nu_\gamma}{230 \text{GHz}} \right) \left(\frac{10^{-19} \text{eV}}{m_a} \right)^2 \left(\frac{B_0}{1 \text{G}} \right)^2 \left(\frac{r}{r_g} \right)$$



Dominant Contribution of Circular Polarization

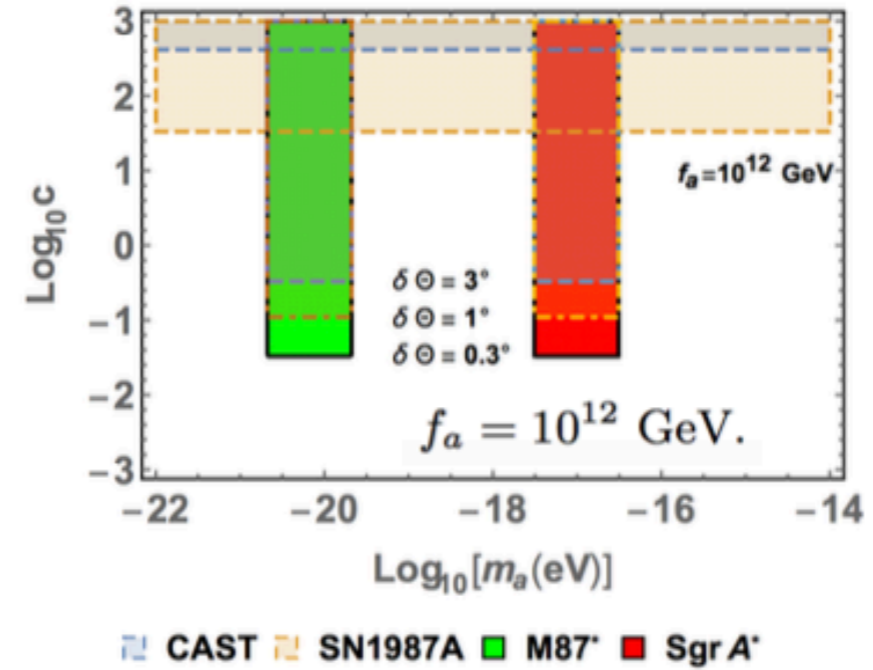
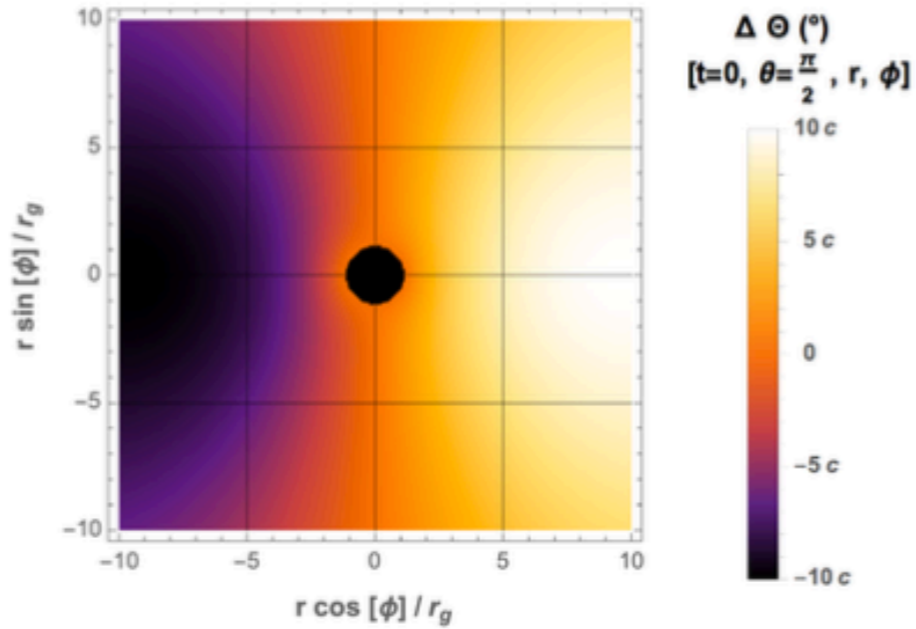
From ALMA (EHT) data we have only a conservative upper bound on the measurement of the circular polarization of M87* at 230 GHz which is around 0.8 %.

$$\Pi_V \equiv \frac{|V|}{I} = |\sin(\Omega t)| \approx |\Omega| t = 0.85 \left(\frac{c_{a\gamma}}{0.1} \right)^2 \left(\frac{\nu_\gamma}{230\text{GHz}} \right) \left(\frac{10^{-19}\text{eV}}{m_a} \right)^2 \left(\frac{B_0}{1\text{G}} \right)^2 \left(\frac{r}{r_g} \right)$$

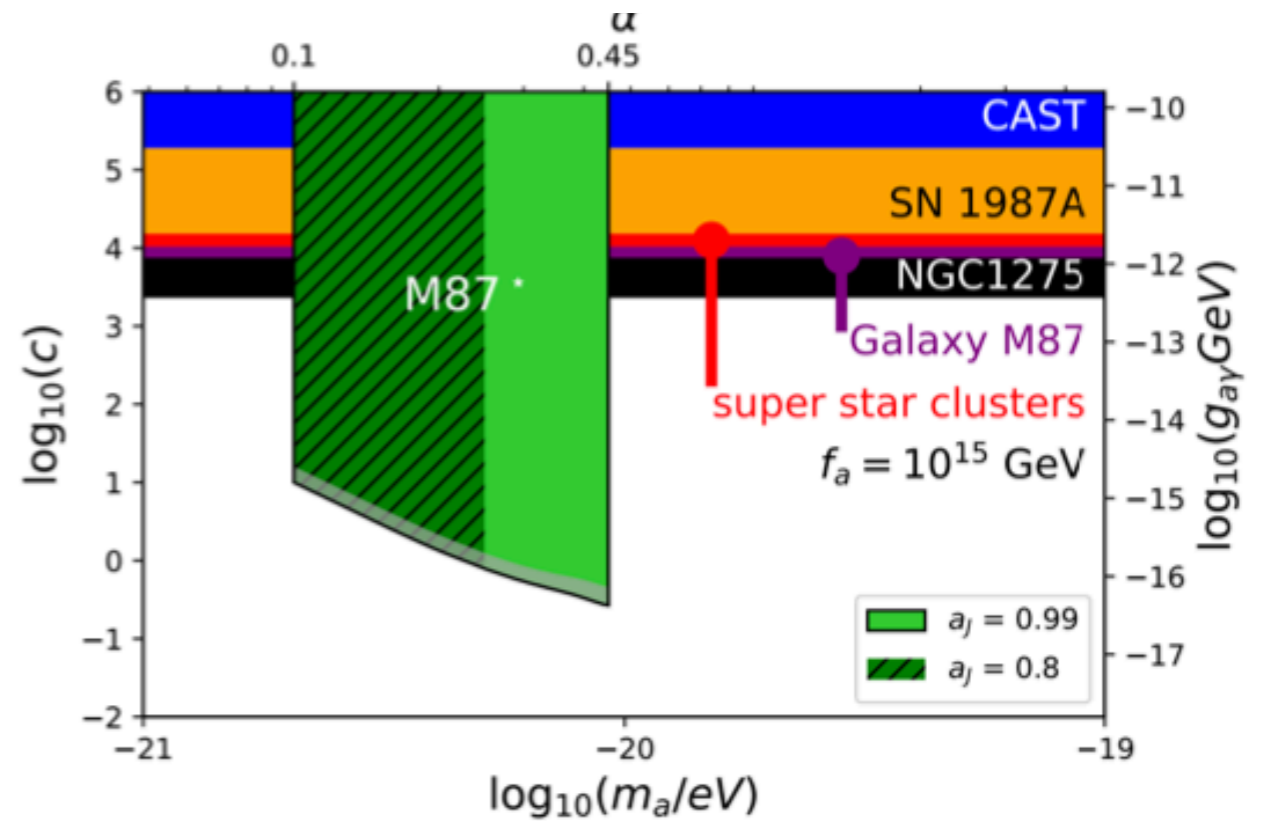
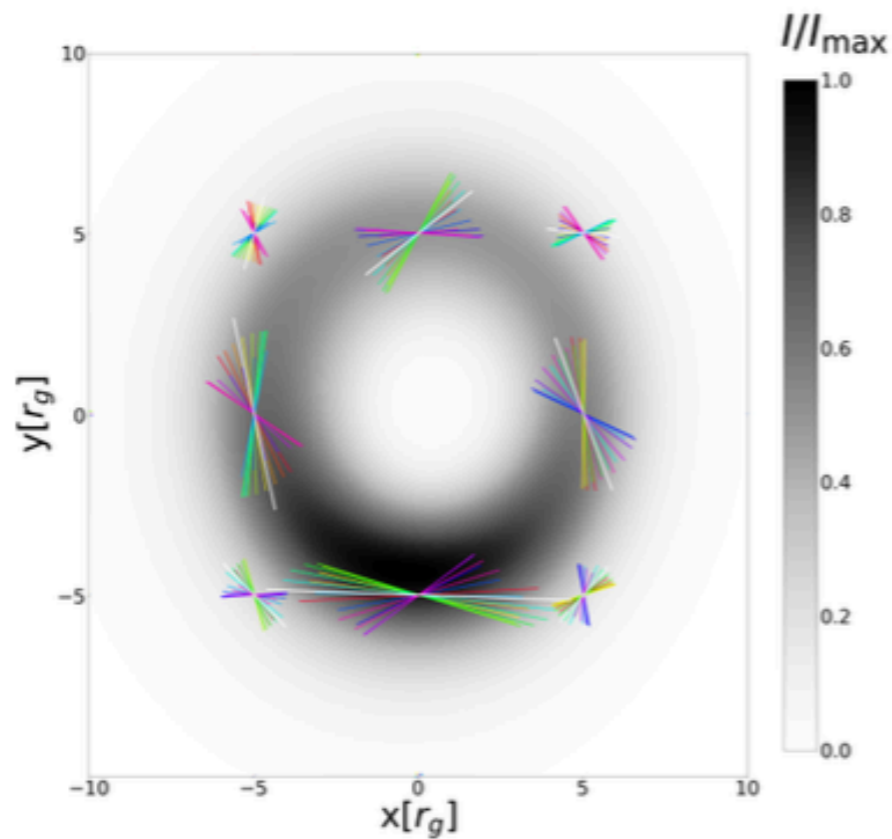


The evolution of Stokes parameters at different distance from the center of black hole are shown in this plot. The initial conditions are $I_0 = 1$, $Q_0 = 1/\sqrt{2}$, $U_0 = 1/\sqrt{2}$ and $V_0 = 0$.

Linear Polarization of Light from EHT and Axion Constraints

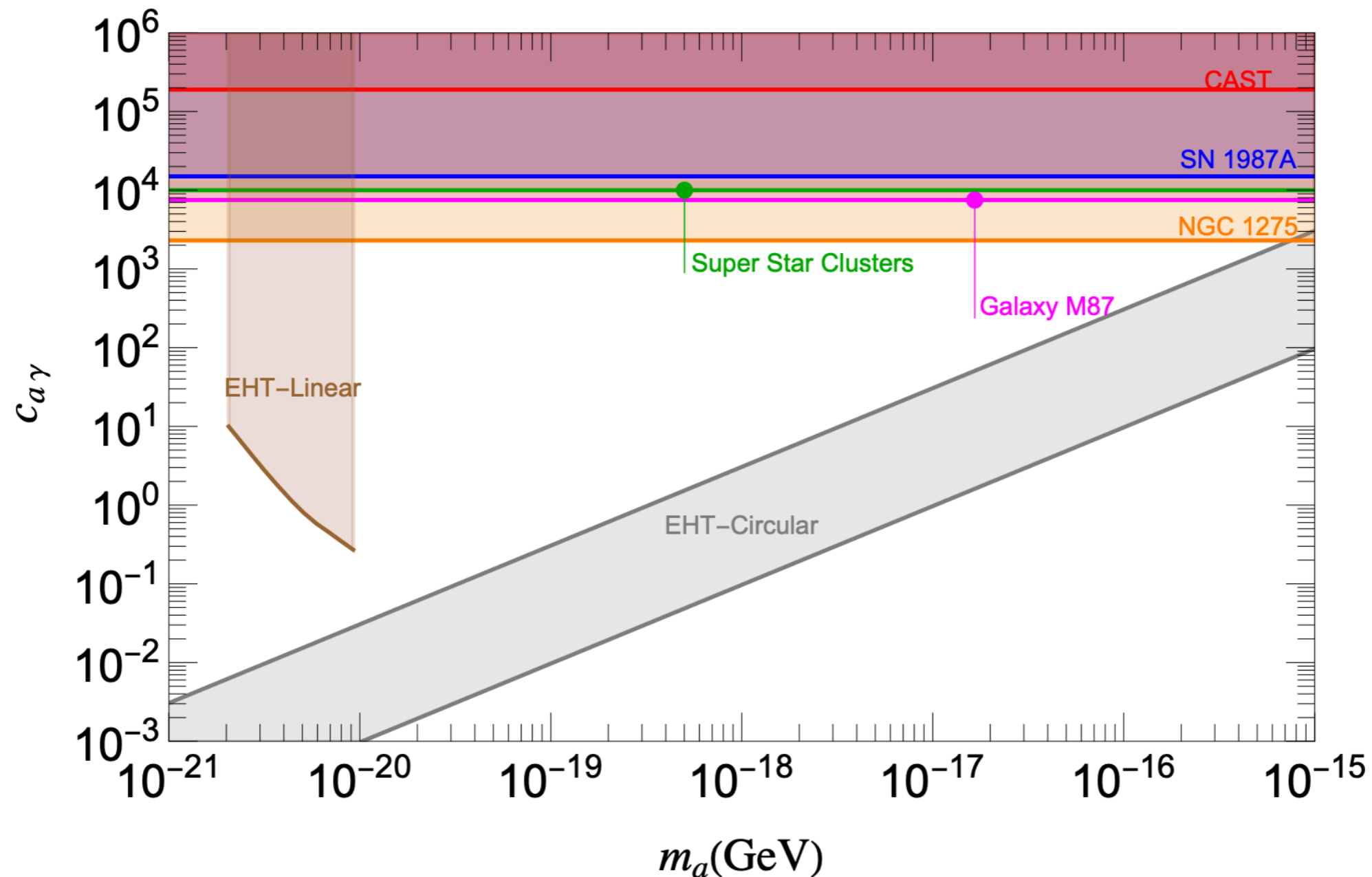


Phys.Rev.Lett. 124 (2020) 6, 061102 • e-Print: 1905.02213



Nature Astron. 6 (2022) 5, 592-598 • e-Print: 2105.04572

Experimental Constraint from Circular Polarization of Light from M87



Constraints on axion mass m_a and its coupling to photons $c_{a\gamma} \equiv 2\pi g_{a\gamma} f_a$ where $f_a = 10^{15} \text{ GeV}$ is assumed. The bound from circular polarization of light from EHT is shown by gray color. Linear polarization of light puts a bound from EHT presented by brown color. The experimental bound from CAST is shown by red color. Astrophysical constraints are also shown.

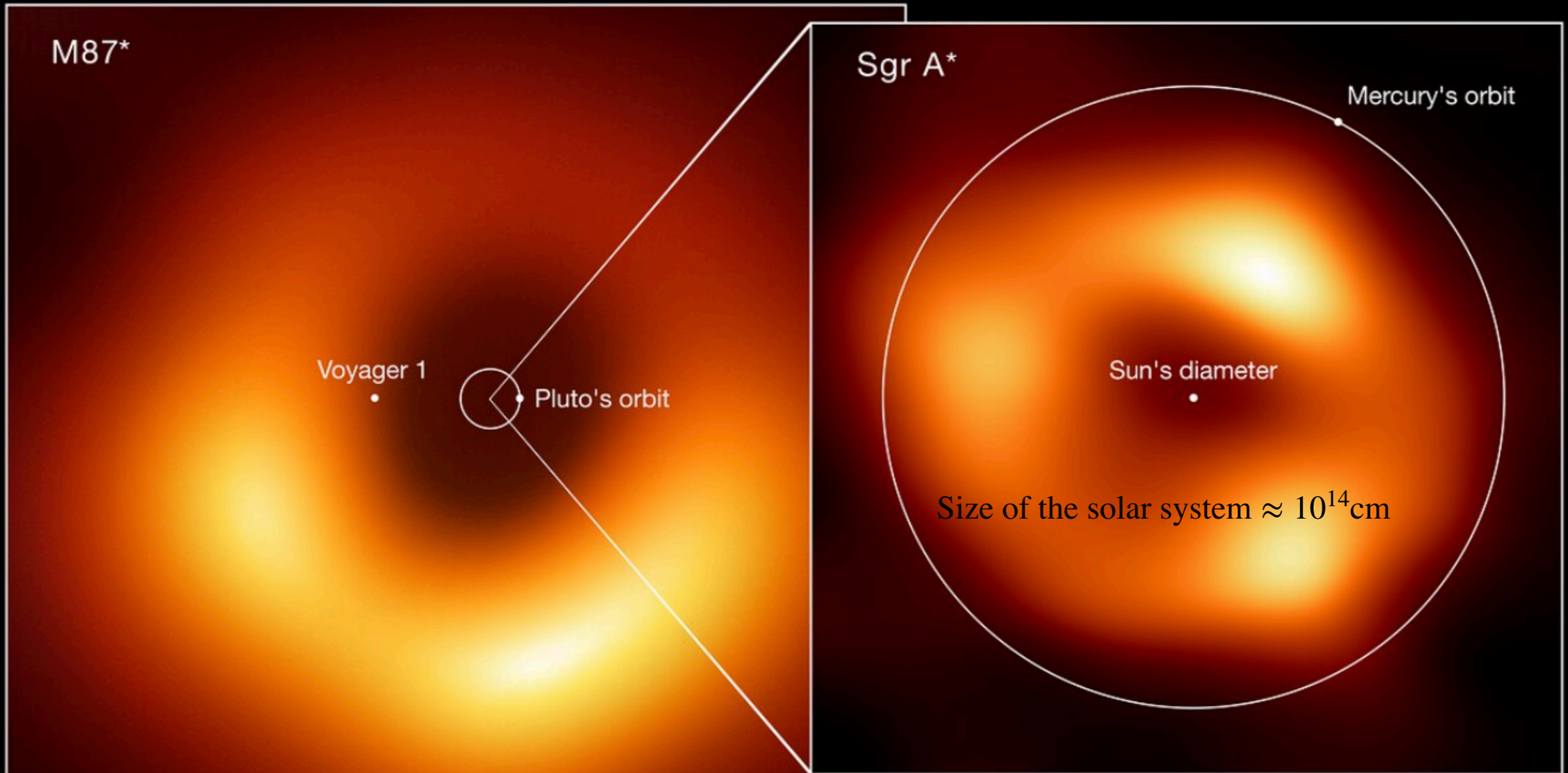
$$m_a \gtrsim 3.27 \times 10^{-19} c_{a\gamma} \left(\frac{\nu_\gamma}{230 \text{ GHz}} \right)^{1/2} \left(\frac{B_0}{\text{G}} \right) \left(\frac{r}{r_g} \right)^{1/2} \text{ eV}$$

[arXiv:2209.13572](https://arxiv.org/abs/2209.13572)

A bright sun is shining through a dense canopy of trees, creating a lens flare effect. The trees are in the foreground, and a house with a chimney and a fence are visible in the background. The scene is set in a residential area with a clear blue sky.

Thanks for your attention!

Size of the Supermassive Black Hole (SMBH) and its Image



$$r_g \equiv GM_{BH} = 2.97 \times 10^{-4} \text{pc} \left(\frac{M_{BH}}{6.2 \times 10^9 M_{\odot}} \right) \quad \boxed{1 \text{pc} = 3.086 \times 10^{18} \text{cm}}$$

The emission region $\sim 5r_g$ The Magnetic Field at the emission region 4.9 G

The electron density $n_e \sim 10^4 \text{cm}^{-3}$ $M_{BH} \approx 6.2 \times 10^9 M_{\odot}$

EVENT HORIZON TELESCOPE collaboration, *First M87 Event Horizon Telescope Results. V. Physical Origin of the Asymmetric Ring*, *Astrophys. J.* **875** (2019) L5 [1906.11242].

C. G. et al., *Polarimetric properties of event horizon telescope targets from alma*, *ApJL* **910** (2021) 54.

E. C. et al., *First m87 event horizon telescope results. vii. polarization of the ring*, *ApJL* **910** (2021) 48.


E. C. et al., *First m87 event horizon telescope results. viii. magnetic field structure near the event horizon*, *ApJL* **910** (2021) 43.

Event Horizon Telescope (EHT)

A Global Network of Radio Telescopes

2017 OBSERVATIONS




ALMA  Atacama Large Millimeter/ submillimeter Array
CHAJNANTOR PLATEAU, CHILE

APEX  Atacama Pathfinder EXperiment
CHAJNANTOR PLATEAU, CHILE

30-M  IRAM 30-M Telescope
PICO VELETA, SPAIN

JCMT  James Clerk Maxwell Telescope
MAUNAKEA, HAWAII

LMT  Large Millimeter Telescope
SIERRA NEGRA, MEXICO

SMA  Submillimeter Array
MAUNAKEA, HAWAII

SMT  Submillimeter Telescope
MOUNT GRAHAM, ARIZONA

SPT  South Pole Telescope
SOUTH POLE STATION

Event Horizon Telescope

